Oleic acid enhances the motility of umbilical cord blood derived mesenchymal stem cells through EphB2-dependent F-actin formation

Young Hyun Jung, Sei-Jung Lee, Sang Yub Oh, Hyun Jik Lee, Jung Min Ryu, Ho Jae Han *

Department of Veterinary Physiology, College of Veterinary Medicine, Research Institute for Veterinary Science, Seoul National University, Seoul 151-741, South Korea
BK21 PLUS Creative Veterinary Research Center, Seoul National University, Seoul 151-741, South Korea

A B S T R A C T

The role of unsaturated fatty acids (UFAs) is essential for determining stem cell functions. Eph/Ephrin interactions are important for regulation of stem cell fate and localization within their niche, which is significant for a wide range of stem cell behavior. Although oleic acid (OA) and Ephrin receptors (Ephs) have critical roles in the maintenance of stem cell functions, interrelation between Ephs and OA has not been explored. Therefore, the present study investigated the effect of OA-pretreated UCB-MSCs in skin wound-healing and underlying mechanism of Eph expression. OA promoted the motility of UCB-MSCs via EphB2 expression. OA-mediated GPR40 activation leads to $G\alpha_q$-dependent $PKC\alpha$ phosphorylation. In addition, OA-induced phosphorylation of $GSK3\beta$ was followed by β-catenin nuclear translocation in UCB-MSCs. Activation of β-catenin was blocked by PKC inhibitors, and OA-induced EphB2 expression was suppressed by β-cateninsiRNA transfection. Of those Rho-GTPases, Rac1 was activated in an EphB2-dependent manner. Accordingly, knocking down *EphB2* suppressed F-actin expression. In vivo skin wound-healing assay revealed that OA-treated UCB-MSCs enhanced skin wound repair compared to UCB-MSCs pretreated with *EphB2*siRNA and OA. In conclusion, we showed that OA enhances UCB-MSC motility through EphB2-dependent F-actin formation involving $PKC\alpha$/$GSK3\beta$/β-catenin and Rac1 signaling pathways.

© 2015 Published by Elsevier B.V.

1. Introduction

Fatty acids are important sources of energy and play a central role in the construction of cell membranes. Fatty acids are classified based on the length of their carbon chain and their degree of saturation. Unsaturated fatty acids (UFAs) are essential for determining stem cell function, and they act as ligands for the G-protein coupled receptor protein GPR40 that, when activated, induces the release of Ca^{2+} from the endoplasmic reticulum into the cytosol [1–3]. Although beneficial effects of UFAs on mesenchymal stem cells (MSCs) have been reported [4], their downstream signaling processes and associated mechanisms have not been fully elucidated. Linoleic acid (LA) and oleic acid (OA) are two UFAs that are abundant in blood plasma. Of those two, OA is the most abundant form of a monounsaturated omega-9 fatty acid (C18:1 cis-9) that is produced by stearoyl CoA desaturase 1 (SCD1), mainly from stearic acid (C18:0) by catalyzing Δ9 desaturation [5]. Moreover, OA has been recognized as an effective biomolecule because it causes MSCs to secrete angiogenic mediators and regulates immunomodulatory functions [4,6,7]. Though the significance of OA with regard to the modulation of stem cell functions has been recognized, the mechanism by which OA mediates beneficial physiological effects at the intracellular signaling level has not been completely described.

Ephrin receptors (Ephs), the largest family of receptor tyrosine kinases (RTKs), are expressed in stem cell niches [8]. There are two classes of these receptors (EphA/EphrinA and EphB/EphrinB) based on their structure and binding affinity [9]. The interaction between Ephs and Ephrins results in bidirectional signal transduction, referred to as forward and reverse signaling, via a cell–cell communication complex that influences the migration and adhesion of cells during development and in the course of wound repair [10–12]. In addition, Ephs have been reported to have ligand- and kinase-independent functions, implying that these receptors can signal in a contact-independent manner [13]. It has also been reported that Ephs play significant roles in a wide range of stem cell behaviors [9]. Moreover, Eph/Ephrin signaling contributes to the recruitment of MSCs into injury sites via the promotion of MSC migration [14,15]. Although the expression patterns of Ephs during developmental progresses have been described, the regulatory mechanism of Ephs has not been fully elucidated in stem cells [16]. A GeneGo MetaCore^TM analysis of UFA-mediated signal pathways

indicates that the expression of several Ephs and Ephrin ligands can be altered by UFAs [17]. Thus, it is possible that OA may alter Eph expression through the transcriptional regulation of gene expression. On this basis, we investigated the microenvironmental transcriptional mechanisms of Ephs. As Ephs play crucial roles in facilitating skin regeneration through epidermal cell migration, proliferation and adhesion [12], we used a skin wound-healing model in this study to examine the relationship between OA and Ephs on the promotion of the therapeutic effects of MSCs.

Therapeutic applications of umbilical-cord-blood-derived MSCs (UCB-MSCs) have been recognized as having promise in the treatment of clinical diseases [18]. UCB-MSCs have multi-lineage differentiation potential and low immunogenicity, and can be isolated from the umbilical cord vein of the placenta after detachment from a newborn [19]. Recently, the transplantation of exogenous MSCs has been used in wound-healing therapies [20,21]. Increased stem cell motility contributes to their therapeutic effects in skin wound-healing [22]; thus, treatment with OA to improve the bioactivity of stem cells is a possible strategy for improving the tissue-regenerative effects of UCB-MSCs. In this study, we investigated the effect of OA on the motility of UCB-MSCs, the skin wound-healing process, and on related signaling pathways.

2. Materials and methods

2.1. Materials

Human UCB-MSCs were provided by Medipost (Seoul, Korea) and use of human UCB-MSCs was approved by the Seoul National University Institutional Review Board (SNUIRB No. E1402/001-001). Isolation and expansion of UCB-MSCs were accomplished according to previous report [23]. OA, hematoxylin, EosinY, U73122, U73343, ethylene-glycol-tetraacetic-acid (EGTA), BAPTA-AM, bisindolylmaleimide-1 (Bis), and staurosporine (Sta), were obtained from Sigma-Aldrich (MO, USA). GW1100 was obtained from Cayman Chemical (MI, USA). F-actin and Cdc42 antibodies were obtained from Abcam (Cambridge, UK). Active-β-catenin antibody was obtained from Millipore. Rac1 antibody was obtained from BD Biosciences (CA, USA). Phospho-pan PKC was acquired from Cell Signaling (MA, USA). EphB2, β-actin, pan-cadherin, α-tubulin, Lamin A/C, total-PKC, PKCα, phospho-PKCα, PKCδ, PKCζ, RhoA, phospho-GSK3β, GSK3β, β-catenin, phospho-cofilin-1, cofilin-1, and profilin-1 antibodies were purchased from Santa Cruz (CA, USA). Oleic acid was diluted in absolute ethanol purchased from Merck Millipore (Darmstadt, Germany). All preparations were made at the moment of use, to avoid oxidation. All reagents were of the highest purity commercially available.

2.2. Culture of UCB-MSCs and adipose tissue derived MSCs

UCB-MSCs were cultured in α-minimum essential medium (α-MEM; Thermo, MA, USA) and penicillin–streptomycin (1%, Gibco, NY, USA), and FBS (10%, Hyclone, UT, USA). Cells were grown in 60- and 100-mm diameter culture plates in an incubator (CO_2 5%, air 95%) at 37 °C. Cells were verified for positive (CD105, CD44, CD166, CD29) and negative (CD90, CD14, CD45, CD34, HLA-DR, Stro-1) surface markers by flow cytometry. We transplanted UCB-MSCs at passage 6 for mouse skin wound-healing assay. Other in vitro experiments have been done at passages 6 to 8. The differentiation potential and karyotypic stability of the UCB-MSCs were confirmed in previous reports where UCB-MSCs provided by Medipost were able to maintain their stemness up to the 11th passage [24]. Culture medium was replaced with fresh α-MEM medium at least 24 h before. After incubation, the cells were rinsed twice with PBS and then maintained in the α-MEM supplemented with indicated agents. To examine the effect of OA on migration of human adipose tissue derived MSCs (AD-MSCs), AD-MSCs were provided by Prof. Kyung Sun Kang (Seoul National University). Cells were cultured in keratinocyte serum

free medium (Invitrogen, CA, USA) supplemented with 0.1 ng/ml EGF, 30 μg/ml bovine pituitary extract and 5% FBS. AD-MSCs at passage 6 were used for migration assay.

2.3. Oris™ cell migration assay

UCB-MSCs were cultured at density of 10^4 cells/0.1 ml in Oris™ stopper well (Platypus Technologies, WI, USA), and incubated until the cell reached around 90% confluence. After serum starvation for 24 h, the stoppers were detached and the wells were rinsed twice with PBS. Cells were incubated with the indicated agents in α-MEM for 24 h and stained with 5 μM calcein-AM (Wako, Osaka, Japan) in PBS for 30 min. Cells that migrated into the detection zone were quantified by measurement of fluorescence using a Victor3 (PerkinElmer, MA, USA). The value of relative fluorescence unit (RFU) in control cells that migrated into the detection zone from the cell seeding zone after 24 h was designed as a control. RFU (100%) represents the normalized values from the control cells that migrated into the detection zone for 24 h.

2.4. In vitro cell migration assay and transwell migration assay

UCB-MSCs were seeded at density of 10^4 cells/0.1 ml on each IBIDI insert dish, which are divided by a 500-μm thick silicone insert (IBIDI, Munich, Germany) and incubated until the cells reached around 90% confluence in culture medium. After serum starvation for 24 h, the silicone inserts were detached and cells were incubated with OA (10 μM) for 24 h or treated with the indicated reagents. To visualize the migrated cells, cells were fixed with 4% paraformaldehyde (PFA) in PBS and stained with Alexa Fluor® 488-phalloidin (1:100, Invitrogen) and pictured by an Olympus FluoView™ 300 confocal microscope with ×100 or ×200 objective. The representative pictures were captured in five random fields of denuded area of triplicate experiments.

Transwell migration assays were carried out using Corning® Transwell® polycarbonate membrane inserts (8 μm pore size, Corning, MA, USA). UCB-MSCs were transfected with EphB2siRNA or NTsiRNA for 24 h and then exposed to OA for 12 h. Trypsinized cells (1×10^5 cells/200 μl) were plated on the upper well and the α-MEM added with 5% FBS was filled in the lower wells. Cells were incubated for 48 h and the cells that migrated to the lower side of the porous membrane were fixed with 4% PFA in PBS and stained with Giemsa. After removing the non-migrated cells with cotton swabs, cells on the bottom side were counted at ×200 magnification and proportional number of migrated cells was evaluated by the percentage of total seeding cells.

2.5. Full thickness skin wound-healing assay

All animal experiments were conducted in accordance with the National Institutes of Health (NIH) Guide for the Care and Use of Laboratory Animals and permitted by Institutional Animal Care and Use Committee (IACUC) of Seoul National University (SNU-140123-6). Male ICR mice (8 weeks old) acquired from Orient Bio (Sungnam, Korea) were used. Mice were anesthetized by 2:1 mixture of Zoletil 50® (20 mg/kg, Virbac, Seoul, Korea) and Rompun® (10 mg/kg, Bayer, Ansan, Korea). Mouse excisional skin wounds were created as described in a report [25]. Two wounds were created separately on the back with sterilized disposable 6-mm-diameter dermal biopsy punch. First, to find the effect of OA-treatment on UCB-MSCs, wounded mice were treated with vehicle or OA, and UCB-MSCs at passage 6 were pre-exposed to vehicle or OA. Second, to investigate the effect of EphB2 expression on UCB-MSC motility in wound area, the cells transfected with NTsiRNA or EphB2siRNA were exposed to vehicle or OA. We injected the same number of cells (1×10^6) in 70 μl of a 1:1 mixture of PBS and Matrigel™ (Growth Factor Reduced, BD Biosciences, CA, USA) into the two sites of dermis around the skin wound and administered topically 3×10^5 UCB-

MSCs in 30 μl with the PBS and matrigel mixture (1:1) on the wound bed on days 0 and 9. After transplantation of UCB-MSCs, the wounds were coated with Tegaderm (3 M Healthcare, Borken, Germany). To examine the extent of tissue repair, mice were anesthetized with isoflurane on days 0, 5, 9, and 12, then, the images of wounds were captured by a camera (D50, Nikon, Japan) at the unchanged height (30 cm) from the mice. The size of wound was determined using Image J with free-hand-selection and represented as the percentage of the initial wound area. For histological and molecular analysis, wound tissues were obtained by using 8-mm-diameter dermal biopsy punch at designated time points. Half of the wound tissue sample was embedded in O.C.T. (Sakura Finetek, CA, USA) and the other half was put in liquid nitrogen before storing in −80 °C freezer for RNA analysis.

2.6. Reverse transcription polymerase chain reaction (PCR) and real time quantitative PCR

Total RNA of UCB-MSCs was extracted by the RNeasy Plus Mini Kit (Qiagen, CA, USA) according to the manufacturer's instructions. To obtain the RNA from skin wound tissue, 30 mg of tissue was minced with blades and homogenized with Rotor-stator homogenizer in provided RLT buffer (Qiagen, CA, USA). Reverse transcription (RT) was conducted with 1 μg of total RNA with a Maxime RT premix kit (iNtRON, Sungnam, Korea). The cDNA was amplified by PCR premix kit (iNtRON) under the conditions: denaturation at 94 °C for 5 min, 32 cycles at 94 °C for 20 s, annealing temperature (AT) for 20 s, and 72 °C for 30 s using MyGenie™ 96 Thermal Block (Bioneer, Daejeon, Korea). Mouse and human primer sequences used for reactions are listed in Supplementary Table 1. β-actin was used for a normalization control gene. Real-time quantification of EphrinB/EphB family was achieved using a Rotor-Gene 6000 (Corbett Research, Cambridge, UK) with a QuantiMix SYBR Kit (PhileKorea, Daejeon, Korea).

2.7. Western blot analysis and subcellular fractionation

Protein concentration was determined by BCA Protein Assay Kit (Pierce, IL, USA). Sample proteins were resolved by SDS-PAGE and transferred to PVDF membranes. The membranes were incubated with the primary antibody at 4 °C for overnight. The specific bands were visualized by ChemiDoc™ XRS + System (Bio-Rad, CA, USA). Subcellular fractionation was conducted by membrane protein extraction kit (ProteoJET™ Membrane Protein Extraction Kit, Fermentas) according to the manufacturer's instructions. The α-tubulin and pan-cadherin were used as markers for cytosolic fraction and membrane fraction, respectively. Nuclear fractionation was performed as previously described [26]. Lamin A/C was used as a marker of nuclear fraction.

2.8. Affinity precipitation

Rac1/Cdc42 Activation Assay and Rho Activation Assay (Millipore) were performed in accordance with the manufacturer's manual. Cells starved for 24 h were exposed to OA and cells were lysed with $1 \times$ MLB buffer. The sample (400 μg) was incubated with Cdc42/Rac binding domain (GST-PAK-PBD) or with the Rho-binding domain of rhotekin (GST-Rhotekin-RBD) at 4 °C overnight. The precipitated proteins were eluted with $2 \times$ laemmli sample buffer and analyzed by western blot.

2.9. Measurement of intracellular calcium mobilization

Changes in intracellular calcium concentrations were monitored using Fluo-3-AM (Invitrogen). Cells cultured in 35-mm-diameter confocal dishes (coverglass–bottom dish, SPL, Korea) were rinsed with PBS. After incubation with Fluo-3-AM (5 μM) for 40 min, cells were rinsed twice with PBS and installed on a perfusion chamber. Fluorescent intensity (488/515 nm) of each cell was attained at 1.8 s intervals using a

confocal microscope with $\times 200$ objective. All analyses of calcium mobilization were analyzed in a single-cell, and the results are expressed as the relative fluorescence intensity (F/F_0).

2.10. Small interfering RNA (siRNA) transfection

Cells were grown until 80% of confluency and transfected for 24 h with target siRNA sequences provided by Dharmacon ON-TARGETplus-SMART-pool siRNA specific for EphB2, β-catenin, $G\alpha_q$, $G\alpha_i$, $G\alpha_{12}$, RhoA, Rac1 and Cdc42 (Dharmacon, CO, USA), or a non-targeting (NT) siRNA (Dharmacon) as a negative control with HiPerFect (Qiagen) according to the manufacturer's guidelines. The siRNA sequences are described in Supplementary Table 2.

2.11. Immunnofluorescence microscopy

Cells were cultured in 35-mm-diameter confocal dishes (SPL) and fixed with 4% PFA in PBS, permeabilized for 5 min with 0.1% (v/v) Triton X-100, and washed each step for three times with PBS for 5 min. Cells were blocked with 5% normal goat serum (NGS, Vector Lab, CA, USA) in PBS for 30 min. Primary antibodies were diluted in 5% (v/v) NGS in PBS at 4 °C overnight. After rinsing with PBS three times for 5 min, cells were incubated with Alexa Fluor 488-(green) and Alexa Fluor 555-(red) secondary antibodies (Invitrogen) for 1 h in RT and counterstained with PI (Invitrogen). Immunostained cells were visualized with a confocal microscope ($\times 100$ and $\times 200$ magnification).

2.12. Immunohistochemical analysis

The OCT-embedded samples were cut into 10-μm thick frozen-sections, and they were mounted on glass slide (Pre-Cleaned Micro Slide Glass, Matsunami, Japan) for staining with hematoxylin and eosin (H&E) and immunohistochemistry. All sections were fixed with 4% PFA in PBS for 10 min and permeabilized for 10 min with Triton X-100 (0.1%) in PBS. 5% NGS in PBS was used for blocking buffer and antibody dilution buffer. Alexa Fluor® 488 conjugated anti-human nuclei antibody (1:100) and PI (1:100) were incubated at RT for 3 h. After washing three times with PBS, slides were coverslipped with Cytoseal-XYL mounting medium (Thermo Fisher Scientific, MA, USA). Images were captured by a confocal microscope ($\times 200$ magnification).

2.13. Cell number counting

UCB-MSCs were grown in 60-mm culture dish until 70% confluency. Cells were synchronized by serum deprivation for 24 h and then exposed to OA. After incubation for indicated time, cells were trypsinized and resuspended in PBS. Cell number was calculated by using a hemocytometer.

2.14. Statistical analysis

Data are presented as means $\pm$ SE and were analyzed by the Student t test for comparing two groups. Results were considered to be statistically significant at $P < 0.05$.

3. Results

3.1. OA increased UCB-MSCs migration and enhanced skin wound-healing effect of UCB-MSCs

To investigate the potential of OA enhancing the bioactivity of stem cells, we initially explored the role of OA on UCB-MSC motility. As shown in Fig. 1A, cells were treated with serial concentrations of OA (0–100 μM) for 24 h. OA promoted the migration of UCB-MSCs at 0.1 to 10 μM compared to vehicle-treated UCB-MSCs. Also, OA stimulated the migration of UCB-MSCs in a time-dependent manner in 12 to 48 h
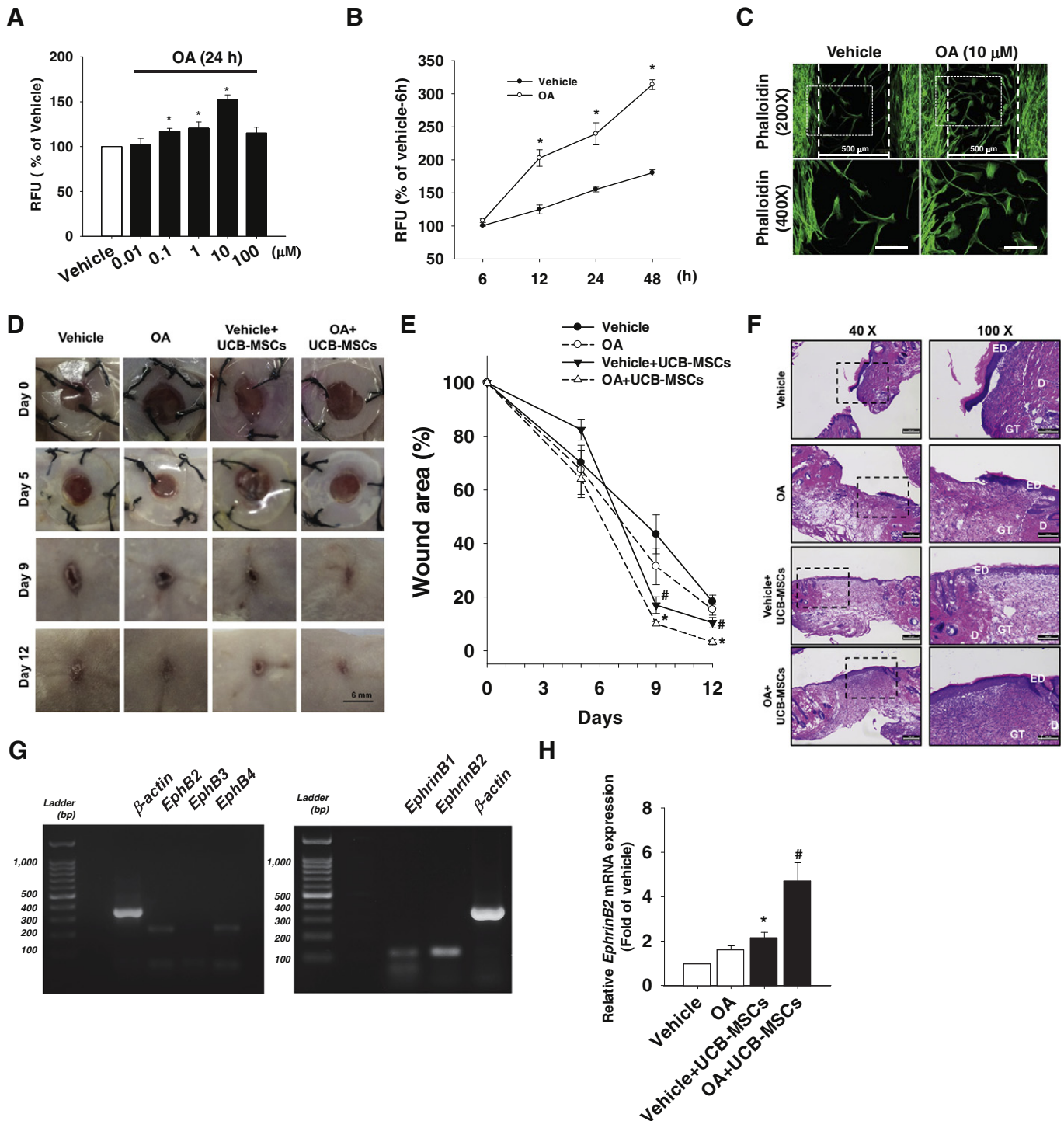
Fig. 1. OA increased UCB-MSC migration and enhanced skin wound-healing effect of UCB-MSCs. (A) Dose response of OA (0–100 μM) on cell migration was measured by Oris™ migration assay after 24 h incubation and cells were stained with calcein-AM. Control means the value of RFU in control cells migrated into the detection zone from the cell seeding zone after removing the uniformed silicone reservoirs for 24 h treatment with vehicle. Data are means ± SE. n = 5. *$P < 0.05$ versus vehicle. (B) Time response of 10 μM OA (6 to 48 h) on UCB-MSC migration was analyzed by Oris™ migration assay. Control means the value of RFU in cells migrated into the detection zone after removing the uniformed silicone reservoirs for each time point treatment with vehicle. n = 5. *$P < 0.05$ versus corresponding time point of vehicle treated group. (C) In vitro cell migration assay. Cells were treated with 10 μM OA or vehicle for 24 h and then stained with Alexa Fluor® 488-phalloidin. n = 3. Scale bar, 500 μm (magnification, ×200) and 100 μm (magnification, ×400) (D) Gross examination on skin wound-healing on days 0, 5, 9 and 12 are shown. n = 8. Scale bar, 6 mm. (E) Percentage of wound area relative to initial wound size on days 0, 5, 9 and 12 are shown. n = 8. *$P < 0.05$ versus vehicle + UCB-MSCs. #$P < 0.05$ versus vehicle alone. (F) Frozen sections of wound tissues were stained with H&E on day 12, and the representative images are shown. Scale bars are indicated as 100 μm (magnification, ×40) and 200 μm (magnification, ×100). ED, epidermis; D, dermis; GT, granulation tissue (G) The mRNA expression of EphB and EphrinB family in mouse wound tissue on day 7 was determined by RT-PCR analysis with mouse specific primers. (H) The mRNA expression of *EphrinB2* was analyzed in vehicle, OA, vehicle + UCB-MSC, and OA + UCB-MSC groups of mice on day 7 by real-time PCR. Total RNA was extracted from mouse skin wound tissues and analyzed as described in Materials and methods. The values are normalized to the corresponding *β-actin* and represented as fold of vehicle. n = 3. Data are means ± SE. *$P < 0.05$ versus vehicle, #$P < 0.05$ versus vehicle + UCB-MSCs.

(Fig. 1B). To confirm the results of OA-enhanced cell migration, proliferation of UCB-MSCs was evaluated by counting the cell number for 72 h. As shown in Supplementary Fig. 1, OA did not have any effect on UCB-MSCs proliferation, indicating that the effect of OA on cell migration is independent of cell proliferation. Moreover, to verify the effect of OA on UCB-MSC motility and visualize the migrated cells, UCB-MSCs were stained with Alexa Fluor® 488-phalloidin, which binds to F-actin. OA significantly increased the number of migrated cells into the gap area compared to the vehicle-treated UCB-MSCs (Fig. 1C). To prove the maintenance of cellular phenotypes, we checked the mRNA expression of differentiation markers for osteoblast (Osteopontin, Runx2), chondrocyte (Sox9, Col2a1), adipocyte (FABP4, PPARγ), and endothelial cell (VE-Cadherin, PECAM1) of the UCB-MSCs at passages 6 and 8 used in this study. Despite the variation of cellular phenotypes and sub-populations, we found that their expression levels were maintained after repeated subcultures (Supplementary Fig. 2). It means that the UCB-MSCs used in our study have maintained their cellular phenotypes. Additionally, to support that our results were not contaminated by contribution of particular MSC subpopulation, we have performed additional experiments to check whether UCB-MSCs remain undifferentiated. The mRNA expression of differentiation markers was not significantly changed for 72 h (Supplementary Fig. 3). In addition, we checked the migration-promoting effect of OA in other sources of MSCs, AD-MSCs. OA significantly stimulated the motility of AD-MSCs (Supplementary
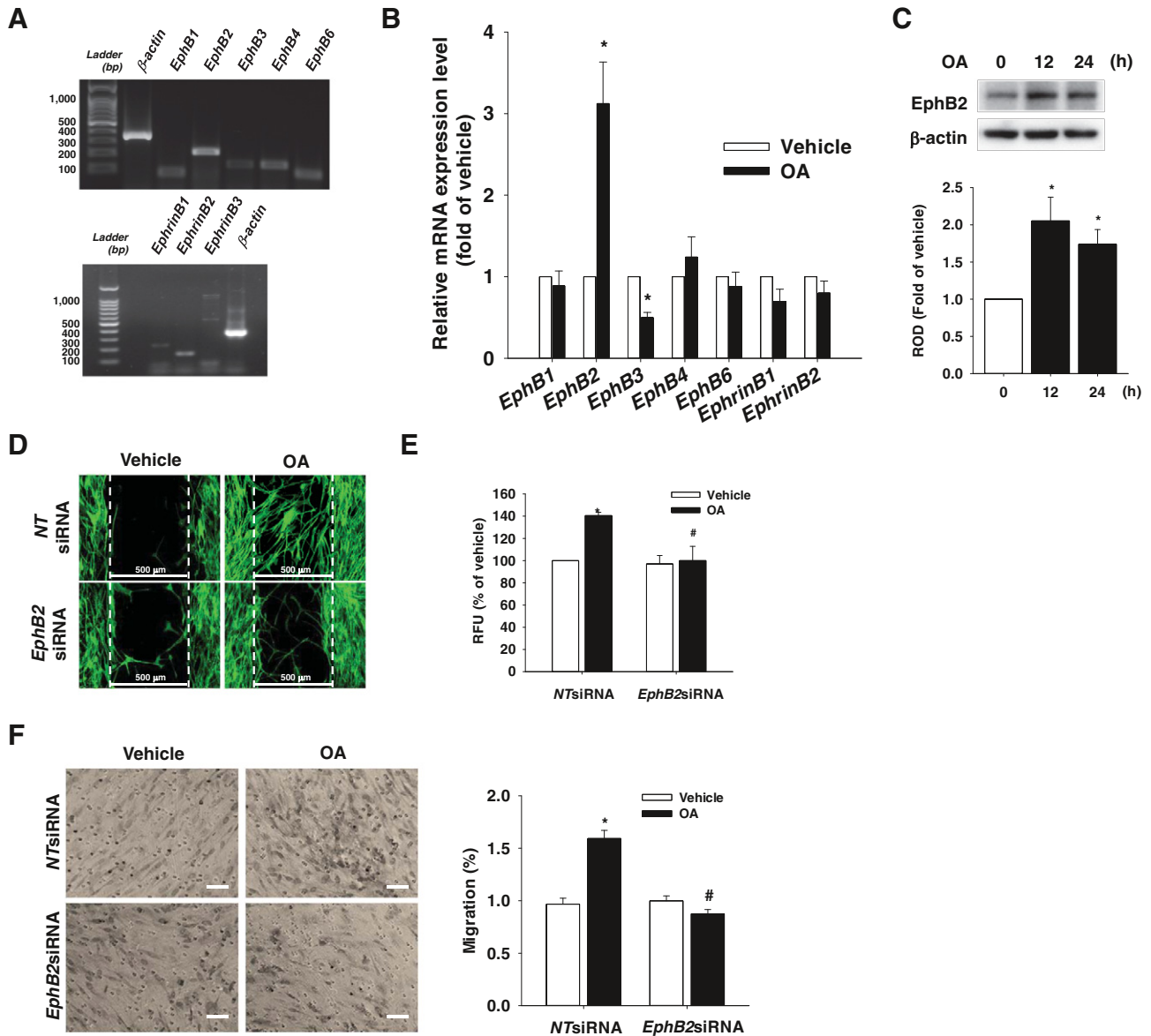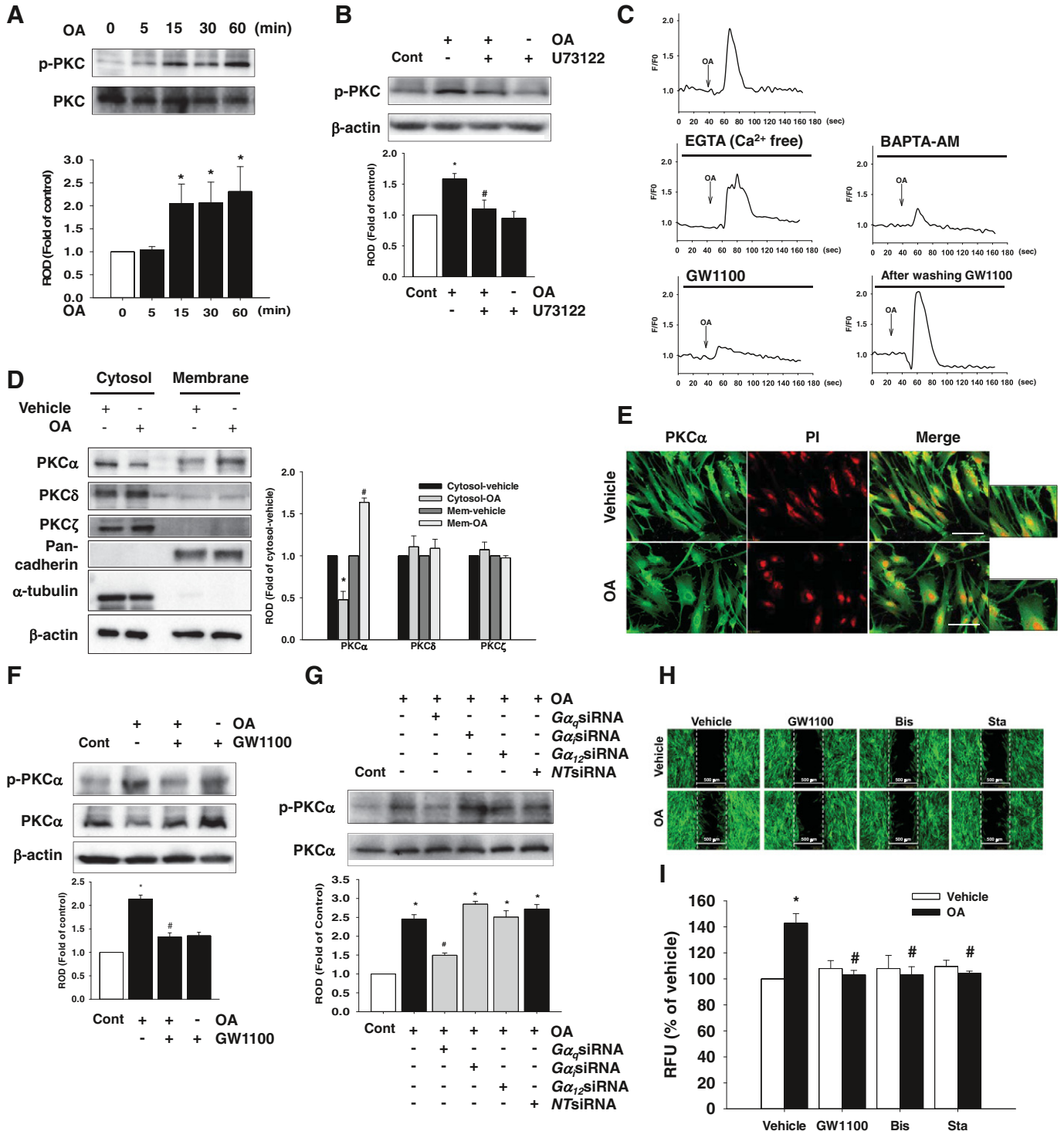

Fig. 2. Effect of OA on the regulation of EphB2 expression in UCB-MSCs. (A) The mRNA expression of the *EphB* and *EphrinB* family was analyzed with RT-PCR. Primers used for PCR are human specific and listed in Supplementary Table 1. (B) Cells were treated with 10 μM OA for 12 h. The mRNA expression of the *EphB* and the *EphrinB* family was quantified by real-time PCR. The results are normalized to the β-actin and represented as fold of vehicle. n = 3. Data are means ± SE. *P < 0.05 versus vehicle. (C) Cells were treated with OA for 12 and 24 h, EphB2 protein expression was determined. β-actin was used as a loading control and RODs are denoted as fold of control. Control is untreated cells. n = 3. Data in bar graphs are means ± SE. *P < 0.05 versus vehicle. (D) In vitro cell migration assay was performed. UCB-MSCs were transfected with *EphB2*siRNA or *NT*siRNA for 24 h and incubated with OA for 24 h. Cells were stained with Alexa Fluor® 488-phalloidin and examined by a confocal microscopy. n = 3. Scale bar, 500 μm (magnification, ×200). (E) Cells were transfected with *EphB2*siRNA or *NT*siRNA for 24 h and then treated with OA for 24 h. The Oris™ migration assay was performed. Control means the value of RFU in cells migrated into the detection zone after removing the uniformed silicone reservoirs for 24 h treatment with vehicle. n = 3. The values are means ± SE. *P < 0.05 versus vehicle + *NT*siRNA. #P < 0.05 versus OA + *NT*siRNA. (F) Cells (1×10^5 cells/200 μl) were plated in upper-chamber and the lower-chamber was filled with a medium (500 μl) containing 5% FBS. After 48 h incubation, Giemsa staining was done. The cells migrated toward lower part were captured by the microscope and counted the number of cells in eight random fields manually. Proportional number of migrated cells was evaluated by the percentage of total seeding cells. Data were acquired from three independent experiments. Scale bar, 100 μm (magnification, ×200). Data are means ± SE. *P < 0.05 versus *NT*siRNA + vehicle, #P < 0.05 versus *NT*siRNA + OA. Abbreviations: bp, base pair; ROD, relative optical density; NT, non-targeting.

Fig. 4). This result indicates that the functional role of OA to induce motility is reproducible in another type of MSC. On the basis of the results that motility of UCB-MSCs could be enhanced by OA, we planned to evaluate the effect of UCB-MSCs and OA. Giving exogenous MSCs a pretreatment of biological molecules improves the efficacy of stem cell transplantation and the skin wound-healing effect. Therefore, we examined the effect of UCB-MSCs pretreated with OA (10 μM) in a mouse skin wound-healing experiment. The wound sizes were considerably decreased in the group that received OA-treated UCB-MSCs compared to the group treated with vehicle, OA and UCB-MSCs treated with vehicle on days 9 and 12 (Fig. 1D). The group given OA-treated UCB-MSCs showed an increased extent of wound closure compared to the other

groups (Fig. 1E). In a histological analysis, the wound region in the mice group given OA-treated UCB-MSCs was recovered by re-epithelialization, and the granulation tissue had completely formed at the wound sites, whereas the skin wound tissue sections of the mice given the vehicle or OA alone were not completely covered by epithelium or granulation tissue (Fig. 1F). In the mouse wound-healing model, EphrinB2 activation is involved in wound-healing and angiogenesis [27]. We investigated the effect of exogenous UCB-MSCs on regulating the expression of Ephrins and their receptors using RT-PCR and real-time quantitative PCR with mouse-specific primers. Among the Ephrins and Eph receptors, EphrinB2 mRNA expression was dominant in mouse skin wound tissue (Fig. 1G). The level of EphrinB2 mRNA expression

was elevated in the group transplanted with OA-preconditioned UCB-MSCs compared to the other groups (Fig. 1H). These results suggest the involvement of EphB receptors in the migration of UCB-MSCs.

3.2. Effect of OA on the regulation of EphB2 expression in UCB-MSCs

To study the effects of exogenous OA-activated UCB-MSCs, we undertook an initial examination of the endogenous expression levels of EphBs and EphrinBs in UCB-MSCs. The results from the RT-PCR analysis showed that the UCB-MSCs expressed *EphB1*, *B2*, *B3*, *B4*, and *B6* as well as *EphrinB1* and *B2*. Among them, the *EphB2* and *EphrinB2* gene expression levels were high in the UCB-MSCs (Fig. 2A). Interestingly, OA increased *EphB2* expression in both the mRNA and protein levels, whereas *EphB3* was decreased in response to OA, but its expression level was too low to detect in UCB-MSCs. In addition, the mRNA expression of *EphrinB2*, a cognate ligand of EphB2, was unaffected by OA exposure (Fig. 2B and C). Because the roles of EphB2 in regulating MSC migration remain controversial [14,28], we examined the function of EphB2 on the motility of UCB-MSCs. To knock down the expression level of *EphB2*, UCB-MSCs were transfected with *EphB2*siRNA and *NT*siRNA and the analysis of *EphB2*siRNA efficacy is presented in Supplementary Fig. 5. An in vitro cell migration assay showed that the reduction of EphB2 expression resulted in decreased UCB-MSC motility in response to OA (Fig. 2D). An Oris™ cell migration assay was also conducted to confirm the role of EphB2 in regulating UCB-MSC migration (Fig. 2E). Furthermore, a transwell migration assay showed that OA pretreatment enhanced UCB-MSC migration ($1.6 \pm 0.07\%$ of total cells) into the lower compartment which added with 5% FBS, whereas the number of cells which migrated to the lower part was reduced by *EphB2*siRNA transfection in spite of the OA pretreatment ($0.88 \pm 0.04\%$ of total cells) (Fig. 2F). These results indicate that OA regulates EphB2 expression and that EphB2 plays a key role in OA-induced UCB-MSC migration.

3.3. Effect of OA on the activation of GPR40 and PKCα

To uncover the mechanism of the regulation of *EphB2* expression of UCB-MSCs, we verified the expressions of GPR40 and GPR120, which are activated by long-chain fatty acids. A RT-PCR analysis showed that *GPR40*, known to be a receptor of OA, was expressed in UCB-MSCs (Supplementary Fig. 6). Given that GPR40 couples with G proteins [29], we analyzed whether OA induces the phosphorylation and translocation of protein kinase C (PKC) isotypes. Phosphorylation of hydrophobic sites on PKC causes PKCs to become primed for activation, which is referred to as PKC maturation [30]. OA increased the phosphorylation of PKC from 15 to 60 min (Fig. 3A). PKC phosphorylation was attenuated by U73122, an inhibitor of phospholipase C (PLC) (Fig. 3B), but U73343,

an inactive analogue of U73122, did not have any significant inhibitory effect on OA-stimulated PKC maturation (Supplementary Fig. 7). Also, OA increased the intracellular Ca^{2+} concentration ($[Ca^{2+}]_i$), as determined by Fluo-3-AM staining (Fig. 3C, top panel on the left). We changed the medium-treated EGTA (0.5 mM) to eliminate the extracellular Ca^{2+} (Ca^{2+}-free) prior to checking the Ca^{2+} influx caused by the OA treatment (Fig. 3C, middle panel on the left). EGTA did not show an inhibitory effect on Ca^{2+} mobilization induced by OA. Moreover, BAPTA-AM was pretreated for 30 min to chelate intracellular Ca^{2+} and the dishes were washed twice with PBS prior to checking the intracellular Ca^{2+} influx by the OA treatment (Fig. 3C, middle panel on the right). BAPTA-AM significantly attenuated OA-induced Ca^{2+} mobilization. These results indicate that intracellular Ca^{2+} mobilization released from endoplasmic reticulum is mainly involved in the OA-mediated signal transduction in UCB-MSCs. Furthermore, we performed experiments to verify the inhibitory effect of GW1100 (GPR40 antagonist) on the OA-mediated intracellular Ca^{2+} mobilization. Interestingly, OA could not induce Ca^{2+} mobilization in the presence of GW1100 (Fig. 3C, bottom panel on the left). However, when GW1100 was washed twice with PBS, OA provoked a mobilization of intracellular Ca^{2+} (Fig. 3C, bottom panel on the right). Thus, these results indicate that the OA-induced intracellular Ca^{2+} mobilization was mediated by the GPR40 activation. In a subcellular fractionation and immunostaining analysis, the membrane translocation of PKCα was observed, whereas those of PKCδ and PKCζ did not occur after an OA treatment for 30 min (Fig. 3D and E). Additionally, OA induced PKCα phosphorylation, which was blocked by GW1100 and *Gαq*siRNA but not by *Gαi*siRNA or *Gα12*siRNA (Fig. 3F and G). This indicates that the activation of Gαq-coupled GPR40 results in the phosphorylation of PKCα. To examine the effects of GPR40 during UCB-MSC migration, cells were pretreated with GPR40 and PKC inhibitors. GPR40 with PKC inhibition blocked OA-induced UCB-MSC migration (Fig. 3H and I). Hence, these results suggest that GPR40-facilitated PKC maturation is involved in OA-mediated signaling pathways and enhances UCB-MSC motility.

3.4. OA regulates EphB2 expression in relation to the GSK3β/β-catenin signaling pathway

Given that calcium-dependent PKC activation leads to glycogen synthase kinase-3β (GSK3β) inactivation and β-catenin nuclear translocation [31], we investigated whether β-catenin signaling may be involved in OA-mediated signal pathways in UCB-MSCs. The accumulation of β-catenin in the nucleus plays important roles in the regulating functions of MSCs, such as proliferation, migration, and differentiation [32], and their effects on EphB expression have been reported [33]. Thus, we further

Fig. 3. Effect of OA on the activation of GPR40 and PKCα. (A) Phosphorylation of PKC in cells treated with OA for 0 to 60 min is shown, which was analyzed in total cell lysates. The band density was normalized to corresponding total PKC and then the RODs were represented as relative value to the control. Control is untreated cells. Data are means ± SE. n = 3. *$P < 0.05$ versus control. (B) Cells were pretreated with U73122 (1 μM) for 30 min and then exposed to OA for 30 min. Phosphorylation of PKC was analyzed by western blot in total cell lysates. The band density was normalized value to corresponding β-actin and then the RODs were calculated as relative to control. Control is cells treated with vehicle for 30 min. Data are means ± SE. n = 3. *$P < 0.05$ versus control. #$P < 0.05$ versus OA alone. (C) Change of $[Ca^{2+}]_i$ in cytosol was determined by Fluo-3-AM (5 μM) staining and captured with a confocal microscope. Cells were exposed to OA for 180 s (top panel on the left). Cells were incubated in media pretreated with EGTA (0.5 mM, calcium chelator) and exposed to OA (middle panel on the left). Cells were incubated with BAPTA-AM (10 μM, intracellular calcium chelator) and washed twice with PBS and exposed to OA (middle panel on the right). GW1100 (10 μM) for 30 min and then exposed to OA (bottom panel on the right). The dishes incubated with GW1100 were washed twice with PBS and cells were exposed to OA (bottom panel on the right). The representative results from three independent experiments were expressed as relative fluorescence intensity at every time point to fluorescence intensity at time 0 (F/F_0) from three independent experiments. (D) Subcellular fraction was performed to examine the translocation of PKC isoforms. Anti-PKCα, δ, and ζ antibodies were used for immunoblotting. Anti-pan-cadherin (membrane) and anti-α-tubulin (cytosol) was used as markers for each fraction. In the right panel, band intensity of PKC isoforms was normalized to pan-cadherin or α-tubulin and expressed as fold of control. Control is the corresponding fraction of cells treated with vehicle for 30 min. Data are means ± SE. n = 3. *$P < 0.05$ versus cytosol-vehicle, #$P < 0.05$ versus membrane-vehicle. (E) PKCα translocation in cells treated with OA is shown by the confocal microscope using immunofluorescence staining with anti-PKCα. Scale bar, 100 μm (magnification, ×200). n = 3 (F) Cells were pretreated with GW1100 for 30 min and exposed to OA for 30 min. Phosphorylation of PKCα was investigated in total cell lysates. The band density was normalized to corresponding PKCα and then the RODs were calculated as relative to control. Control is cells treated with vehicle for 30 min. Data are means ± SE. n = 3. *$P < 0.05$ versus control. #$P < 0.05$ versus OA alone. (G) Cells were transfected with *Gαq*, *Gαi*, *Gα12*, and *NT*siRNA for 24 h and exposed to OA for 30 min. Phosphorylation of PKCα was examined in total cell lysates. The band density was normalized to corresponding PKCα and then the RODs were calculated as relative to control. Control is cells treated with vehicle for 30. Data are means ± SE. n = 3. *$P < 0.05$ versus control. #$P < 0.05$ versus OA alone. (H) In vitro cell migration assay was done. Cells were pretreated with GW1100 (10 μM), Bis (1 μM) and Sta (100 nM) for 30 min and incubated with OA for 24 h. Cells were stained with Alexa Fluor® 488-phalloidin. n = 3. Scale bar, 500 μm (magnification, ×100). (I) Oris™ migration assay was done. Data were calculated as described in Materials and methods. Control is the cells treated with vehicle for 24 h. Data are means ± SE. n = 3. *$P < 0.05$ versus vehicle. #$P < 0.05$ versus OA alone. Abbreviations: PKC, protein kinase C; ROD, relative optical density; EGTA, ethylene glycol tetraacetic acid; RFU, relative fluorescence unit; NT, non-targeting; Bis, bisindolylmaleimide; Sta, staurosporine.

investigated the effect of OA on β-catenin nuclear translocation. GSK3β phosphorylation and the active form of β-catenin (ABC) were increased for 15 to 60 min in response to OA (Fig. 4A). A fractionation assay of nuclear and non-nuclear fractions showed that the nuclear accumulation of β-catenin was triggered by the OA treatment after 60 min (Fig. 4B). To confirm the effect of OA on β-catenin nuclear translocation, immunofluorescence staining was conducted by staining with PI and ABC. After an OA treatment for 60 min, ABC was detected in the nucleus part (Fig. 4C), but OA-induced GSK3β phosphorylation and the nuclear translocation of β-catenin were inhibited by the PKC inhibitors bisindolylmaleimide-1 (Bis) and staurosporine (Sta) (Fig. 4D). To verify the transcriptional regulation of β-catenin during EphB2 expression, UCB-MSCs were transfected with β-cateninsiRNA before the OA treatment. As indicated in Fig. 4E, the expression of EphB2 was reduced by the knock-down of β-catenin despite the OA treatment. In addition, OA-induced UCB-MSCs migration was blocked by the suppression of β-catenin expression in both the in vitro cell migration assay (Fig. 4F) and the Oris™ migration assay (Fig. 4G). These results suggest that OA-induced EphB2 expression is regulated via GSK3β/β-catenin signaling and plays a role in enhancing the migration of UCB-MSCs.

3.5. EphB2 regulates F-actin expression and the migration of UCB-MSCs

EphB2 forward signaling affects cytoskeletal reorganization by modulating Rho GTPases, such as RhoA, Rac1 and Cdc42, which are important for assembling branches of actin filaments in motile cells [34]. To examine the role of EphB2 on F-actin polymerization, we evaluated the F-actin expression and activity of the actin-binding protein in UCB-MSCs. F-actin was increased after 8 h incubation. Also, the expressions of profilin-1 and phosphorylation of cofilin-1 arose in conjunction with F-actin expression after 8 h of incubation (Fig. 5A). OA also increased the translocation of EphB2 into the membrane with the expression of F-actin in the UCB-MSCs (Fig. 5B). However, the silencing of EphB2 expression by EphB2siRNA hindered OA-induced F-actin expression (Fig. 5C). To determine the role of OA in the activation of Rho GTPases, UCB-MSCs were stimulated by OA for 12 h and then precipitated with GST-PAK-PKB and GST-Rhoteckin-RBD. The GTP-bound Rac1 was specifically increased by OA, but Cdc42 or RhoA were not involved in promoting F-actin reorganization in response to OA (Fig. 5D). To confirm the role of EphB2 in regulating the activity of Rho GTPases, UCB-MSCs were transfected with EphB2siRNA and the cells were exposed to OA for 12 h. Interestingly, OA-induced Rac1 activation was compromised in the EphB2siRNA transfected UCB-MSCs regardless of the OA treatment (Fig. 5E). After an OA treatment for 12 h, Rac1 translocation to the leading edges and the lamellipodia region was observed (Fig. 5F). To determine the involvement of Rac1 activation in the OA-induced migration of UCB-MSCs, the UCB-MSCs were transfected with Rac1siRNA. The OA-induced migration of UCB-MSCs was blocked by the transfection of Rac1siRNA, but this was independent of RhoA or Cdc42 expression levels (Fig. 5G and H). Therefore, these data suggest that OA-induced EphB2 expression contributes to the rearrangement of F-actin and the UCB-MSC migration via Rac1 activation.

3.6. OA-induced EphB2 expression enhances the skin wound-healing effect of UCB-MSCs

We have shown that the migration of OA-treated UCB-MSCs is related to EphB2 expression in vitro. To examine the direct relationship between EphB2 expression and the skin wound-healing effect, an in vivo skin wound-healing assay was conducted through the transplantation of UCB-MSCs transfected with EphB2siRNA or NTsiRNA. The UCB-MSCs were transplanted into the wound sites. From day 9, the remaining wound size of the OA-treated NTsiRNA + UCB-MSC group was significantly smaller than that of the OA-treated EphB2siRNA + UCB-MSC group, as determined by gross examinations of the wound sizes (Fig. 6A and B). Consistent with this, a histological examination on day 12

indicated that the wound beds were filled with granulation tissues in the OA-treated NTsiRNA + UCB-MSC group, whereas the structures of the epidermis and dermis were not completely repaired in the OA-treated EphB2siRNA + UCB-MSC group (Fig. 6C). On day 12, to confirm the relationship between EphB2 expression and OA-induced UCB-MSC migration in vivo, frozen sections of wound tissue were stained with Alexa Fluor® 488 conjugated anti-human nuclei antibody (MAB1281A4, clone 235-1, Millipore) which is a human-specific antibody. Preconditioning UCB-MSCs with OA increased the number of NTsiRNA + UCB-MSCs in the wound bed as compared to the number of EphB2siRNA + UCB-MSCs (Fig. 6D). These results signify the involvement of EphB2 in the enhancement of UCB-MSC migration into the wound bed and promoting the wound-healing effect of UCB-MSCs through preconditioning with OA.

4. Discussion

Our results show that OA enhances UCB-MSC motility through EphB2-dependent F-actin expression. In this study, we investigated the effect of OA-treated UCB-MSCs on stem cell migration to wound sites during skin wound-healing using an in vivo skin wound-healing model. The results indicate that UCB-MSCs pretreated with OA enhance re-epithelialization and more efficiently repair the epidermis compared to those obtained from UCB-MSCs pretreated with vehicle. Through an mRNA expression analysis, we observed that EphrinB2 expression was dominant within the EphB/EphrinB family in mouse skin tissue. Moreover, the level of expression increased with the degree of wound repair. EphrinB2 is required for vascular development and plays crucial roles in angiogenesis, which is regulated by microenvironmental factors such as changes in oxygen tension and which is affected by angiogenic factors in the wound region [35–37]. Therefore, an increase in EphrinB2 expression can promote wound recovery, and EphrinB2 and EphB interaction may play an important role in the skin wound-healing process. On this basis, we investigated the effect of OA on UCB-MSC migration and the association between OA and the expression of EphBs. The results revealed that EphB2 expression was the highest among the EphBs expressed in UCB-MSCs. Moreover, OA uniquely increased EphB2 expression, which was involved in OA-induced UCB-MSC migration. Our results are supported by a report showing that EphB/EphrinB regulates the migration of neural progenitor cells and that controlling their expression may be useful in the treatment of brain injuries or neurodegenerative diseases [38]. In addition, the EphB2 expression level determines the functional activity levels of stem cell migration and proliferation [39]. However, the mechanism of the OA-mediated migration of UCB-MSCs has not been fully elucidated.

Extracellular OA activates GPR40 [40], but the role of GPR40 in UCB-MSCs has not been investigated. Recent reports have shown that OA regulates gene expression via GPR40-dependent conventional PKC activation [41,42]. In addition, GPR40 induces diverse signaling across the plasma membrane, and it has been reported that GPR40 couples with the heterotrimeric G proteins $G\alpha_q$, $G\alpha_i$, and $G\alpha_s$ to modulate insulin secretion [43]. The $G\alpha_q$-dependent PLC activation leads to the cleavage of phosphatidylinositol 4,5-bisphosphate (PIP_2) into inositol triphosphate (IP_3) and diacylglycerol (DAG), which results in a release of Ca^{2+} from the ER into the cytosol [45]. Newly synthesized PKCs should be matured to be activated via a series of phosphorylation at the activation loop site and hydrophobic motif in the C-terminal of the PKC [44]. In this study, we found that OA phosphorylates the hydrophobic sites of the PKCs in a time-dependent manner, which determines the final step of maturation for reaching maximal enzymatic effects. Especially, PKC maturation was also regulated by OA-induced PLC activation dependently. Among the PKC isoforms, OA provoked the translocation of conventional PKCα. Consistently, we showed that the OA-induced intracellular Ca^{2+} mobilization was initiated by GPR40 receptor activation and independently regulated by the extracellular Ca^{2+} concentration. Because PKCα is a conventional PKC that requires both Ca^{2+} and DAG for activation [46], Ca^{2+} binding to the C2 domain of matured PKCα initiates
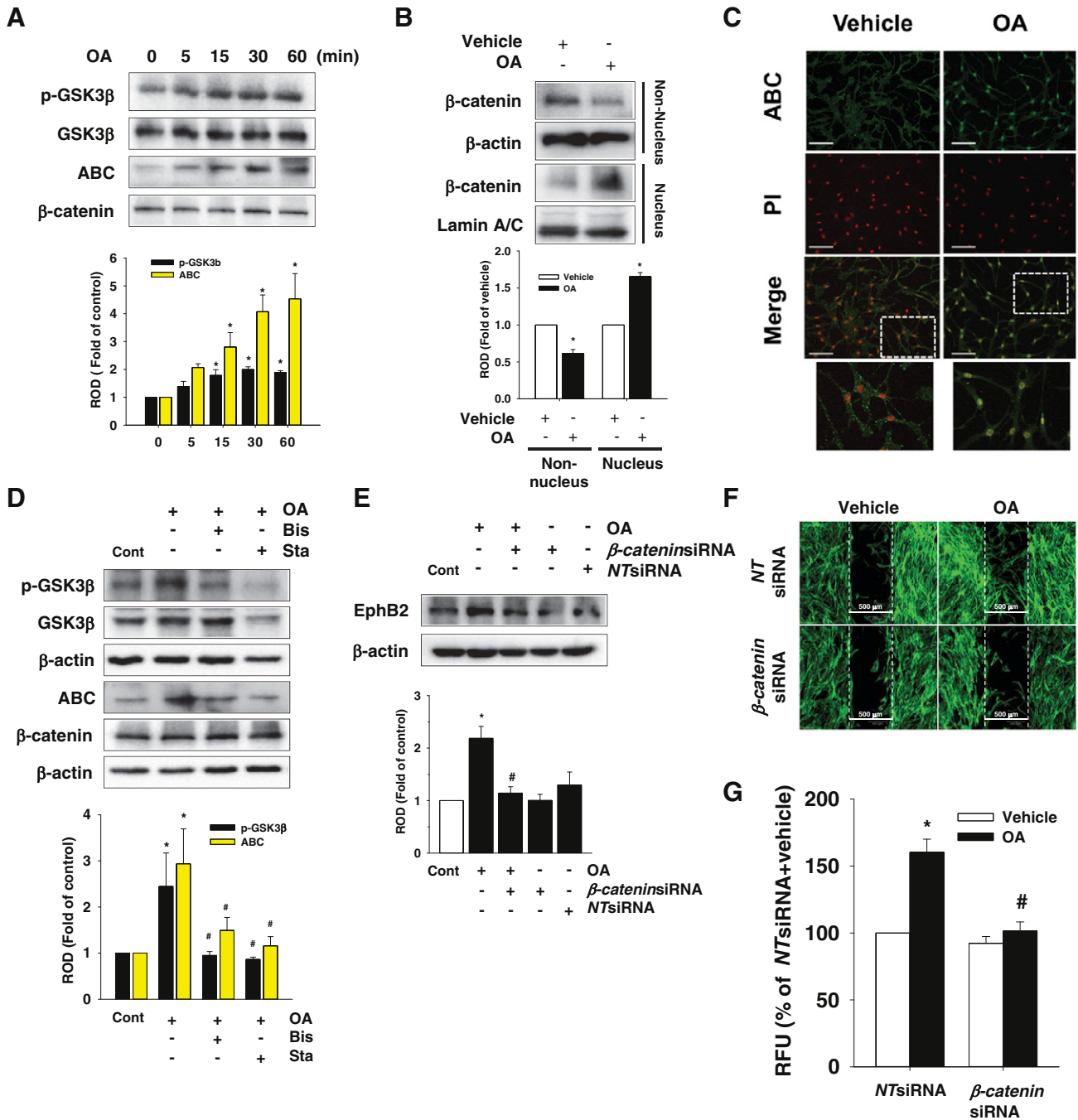
Fig. 4. OA regulates EphB2 expression in relation to the GSK3β/β-catenin signaling pathway. (A) Phosphorylation of GSK3β and activation of β-catenin were analyzed by western blot. The cells were treated with OA (10 μM) for 0 to 60 min. The band density was normalized to total-GSK3β or β-catenin and then the RODs were represented as relative value to the control. Control is untreated cells. Data are means ± SE. n = 3. *$P < 0.05$ versus control. (B) Translocation of β-catenin into the nucleus was determined by subcellular fractionation. The cells were stimulated with OA for 60 min, and nuclear protein was extracted from the cells. The band density was normalized to β-actin or Lamin A/C and then the RODs were represented as relative value to the control. Control is cells treated with vehicle for 60 min. Data are means ± SE. n = 3. *$P < 0.05$ versus control. (C) The cells were treated with OA for 60 min. Cells were immunostained with anti-ABC antibody (Green) and PI (Red), then analyzed by a confocal microscope. Scale bar, 100 μm (magnification, ×100), n = 3. (D) Effect of PKC inhibition on phosphorylation of GSK3β and activation of β-catenin was determined by western blot analysis. Cells were pretreated with Bis (1 μM) and Sta (100 nM) and exposed to OA for 60 min. The band density was normalized to β-actin and then the RODs were represented as relative value to the control. Control is cells treated with vehicle for 60 min. Data are means ± SE. n = 3. *$P < 0.05$ versus control, #$P < 0.05$ versus OA alone. (E) Cells were transfected with β-cateninsiRNA (25 nM) or NTsiRNA (25 nM) for 24 h, and then exposed to OA for 24 h. EphB2 expression was analyzed by western blot using an anti-EphB2 antibody. The band density was normalized to β-actin and then the RODs were represented as fold of control. Control is cells treated with vehicle for 60 min. Data are means ± SE. n = 3. *$P < 0.05$ versus control, #$P < 0.05$ versus OA alone. (F) In vitro cell migration assay was conducted. Cells were transfected with β-cateninsiRNA or NTsiRNA for 24 h and incubated with OA for 24 h. Scale bar, 500 μm (magnification, ×100). n = 3. (G) Oris™ migration assay was carried out. Data were calculated as described in Materials and methods. Control is the cells treated with NTsiRNA + vehicle for 24 h. Cells were transfected with β-cateninsiRNA or NTsiRNA for 24 h and incubated with OA for 24 h. Data were normalized to fluorescent signal of the NTsiRNA + vehicle. Data are means ± SE. n = 3. *$P < 0.05$ versus NTsiRNA + vehicle. #$P < 0.05$ versus NTsiRNA + OA. Abbreviations: GSK, glycogen synthase kinase; ABC, active-β-catenin; PI, propiodium iodide; Bis, bisindolylmaleimide; Sta, staurosporine; NT, non-targeting; ROD, relative optical density; RFU, relative fluorescence unit.

translocation to the membrane. And several studies have reported that PKCα activation plays a crucial role in the migration of cord-blood-derived stem cells [47,48]. Related to this, OA-induced PKCα phosphorylation was inhibited by a GPR40 antagonist, GW1100, and controlled by $G\alpha_q$, but not by $G\alpha_i$ or $G\alpha_{12}$. Our results suggest that OA-induced GPR40 activation leads to Ca^{2+}/DAG-dependent PKCα membrane translocation and regulates the gene expression of UCB-MSCs. Subsequently, PKC regulates GSK3β phosphorylation and results in the

inactivation of GSK3β [49], inhibiting the degradation of β-catenin. The nuclear translocation of β-catenin is a determinant of the expression of some genes [50]. In the present study, the OA-induced phosphorylation of GSK3β led to nuclear translocation and the accumulation of β-catenin in UCB-MSCs. Our observations are supported by a report showing that β-catenin nuclear translocation is impaired by the inhibition of OA production in breast cancer cells [51]. Our results indicate that OA regulates β-catenin-mediated target
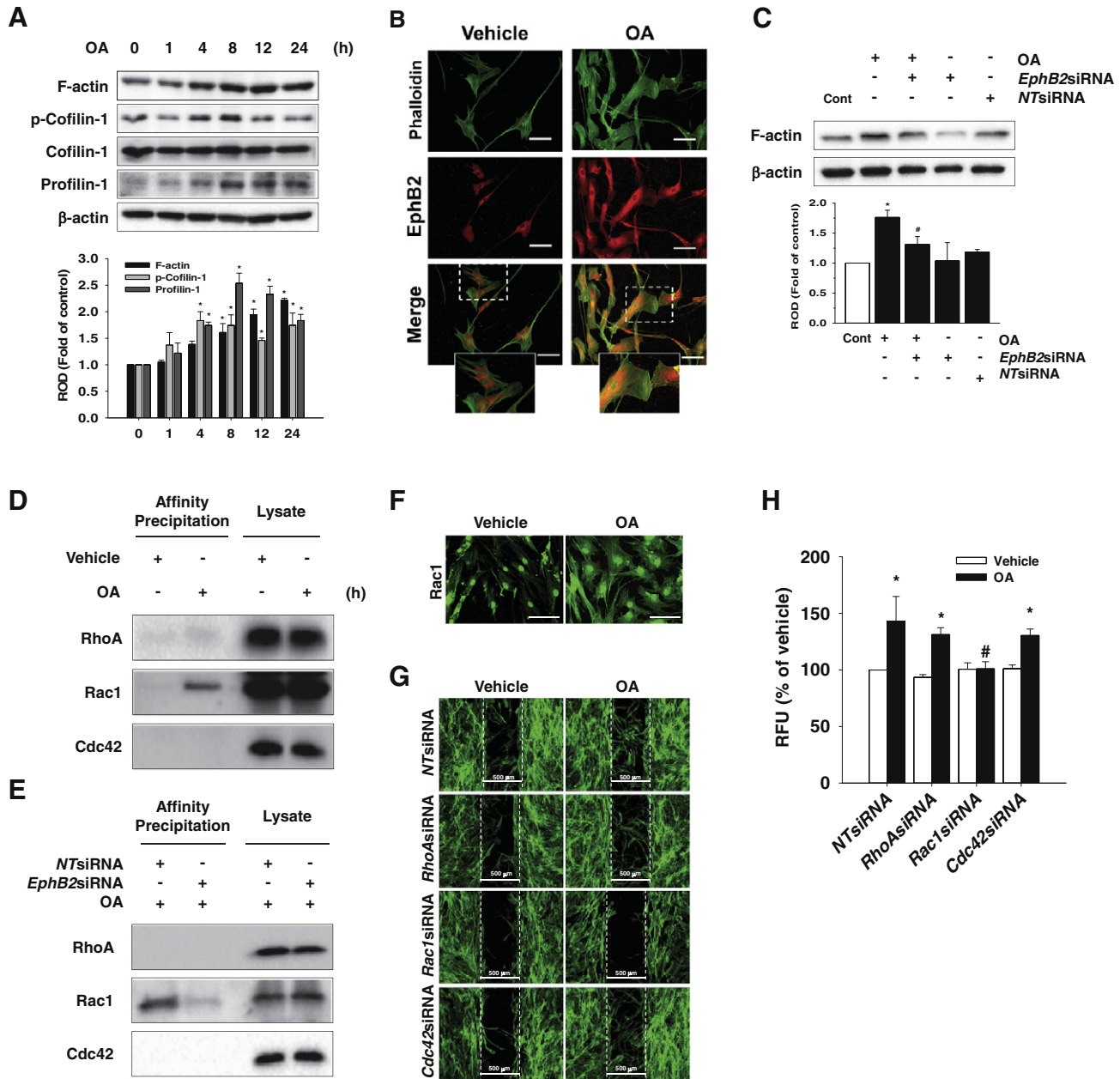

Fig. 5. EphB2 regulates F-actin expression and the migration of UCB-MSCs. (A) The cells were incubated with OA for 0 to 24 h. Total cell lysates were analyzed by western blotting. Their expressions were determined by densitometry and β-actin was used as a loading control. RODs are denoted as fold of control. Control is cells treated with OA for 0 h. Data are means ± SE. n = 3. *P < 0.05 versus control. (B) Expression of F-actin and EphB2 was determined by immunostaining with Alexa Fluor® 488-phalloidin and anti-EphB2 antibody. Cells were treated with OA for 12 h and examined by a confocal microscope. Scale bar, 50 μm (magnification, ×400). n = 3. (C) Cells were transfected with *EphB2*siRNA or *NT*siRNA for 24 h and incubated with OA for 24 h. The expression of F-actin was detected by anti-F-actin antibody. Data were normalized to β-actin and expressed as fold of control. Control is cells treated with vehicle for 24 h. n = 3. Data are means ± SE. *P < 0.05 versus vehicle. #P < 0.05 versus OA alone. (D) Cells were treated with OA for 12 h, and pull-down assays were conducted as described in Materials and methods to precipitate GTP-bound form of Rac1, Cdc42, and RhoA. GTP-Rac1, -Cdc42, and -RhoA were immunoblotted using their specific antibodies. (E) Cells were transfected with *NT*siRNA or *EphB2*siRNA and incubated with OA for 12 h, and pull-down assays were conducted. (F) Cells were treated with OA for 12 h. Rac1 was immunostained with anti-Rac1 antibody and visualized with a confocal microscope. Scale bar, 100 μm (magnification, ×200). (G) In vitro wound healing assay was performed. Transfection of *RhoA*-, *Rac1*-, and *Cdc42*siRNA for 24 h was performed prior to incubation with OA for 24 h. Scale bar, 500 μm (magnification, ×100). n = 3. (H) Oris™ migration assay was conducted. Data were calculated as described in Materials and methods. Control is the cells treated with *NT*siRNA + vehicle for 24 h. Data are means ± SE. n = 3. *P < 0.05 versus *NT*siRNA + vehicle, #P < 0.05 versus *NT*siRNA + OA. Abbreviations: NT, non-targeting; ROD, relative optical density; RFU, relative fluorescence unit.

gene expression in UCB-MSCs. In addition, it has been reported that Wnt/β-catenin signaling regulates EphB2 expression [33]. In this study, we showed that OA-induced EphB2 expression was suppressed by β-cateninsiRNA transfection in UCB-MSCs and that their motility was reduced by the knock-down of β-catenin. Therefore, we suggest that an OA signaling axis of PKCα/GSK3β/β-catenin mediates the transcriptional regulation of EphB2 expression. Our results indicate that when UCB-MSCs are pretreated with OA, their bioactivity is enhanced through changes in EphB2 expression.

The roles of EphB2 in the developmental process and during neuronal migration have been studied [52], but determining the role of EphB2 in promoting the migration of UCB-MSCs has remained elusive. Thus, we attempted to identify how EphB2 regulates the migration of UCB-MSCs by investigating the effect of EphB2 expression on cytoskeletal changes. Our results showed that cofilin-1 and profilin-1 were involved in OA-induced F-actin reorganization. A recent study of the importance of EphB2 in regulating cytoskeletal rearrangements showed that EphB2 overexpression, in cooperation with focal adhesion kinase activation, is related to the migration and invasiveness of glioblastomas [34]. Our results show that the functional effects of OA-induced EphB2 on F-actin reorganization are related to cell motility. When we knocked down EphB2 expression, F-actin expression was reduced. In addition, our results showed that OA-induced EphB2 expression results in the activation of Rac1, but not RhoA or Cdc42, in UCB-MSCs. Localized Rac1 activation controlled by RTKs causes the formation of lamellipodia and directed cell migration [53,54]. In particular, the EphB2-dependent recruitment of kalirin-7, one of the guanine nucleotide exchange factors (GEFs), is associated with the activation of Rac1 and regulates actin polymerization via the Arp2/3 complex in hippocampal neurons [55]. Our results suggest that OA-induced EphB2 expression mediates the downstream signal pathways involved in the activation of Rac1; however, the precise mechanism requires further investigation. Furthermore, a cytoskeletal rearrangement accompanies stem cell migration to an injury site in response to wound-healing mediators such as proinflammatory cytokines, chemokines, and angiogenic factors [56,57]. We observed that an OA pretreatment improved the migration ability of UCB-MSCs and increased the number of UCB-MSCs at wound sites. Thus, we suggest that EphB2 expression contributes to the enhancement of UCB-MSC motility and engraftment. Previously, it was reported that endogenous EphB2/B4 activation enhances chemotaxis in endothelial cells [58]. Although it remains controversial, because EphB/EphrinB contact-dependent repulsion behavior appears during the modulation of cell sorting [59], it appears that OA-induced EphB2 expression can impart the ability to migrate to wound sites in UCB-MSCs. A high level of EphB2 expression is reported to enhance the homing and engraftment of human bone marrow stromal cells [15]. Our results indicate that OA-induced EphB2 expression is important for UCB-MSC migration both in vitro and in vivo. The involvement of MSCs in skin wounds suggests a role of MSCs in the serial processes of wound healing via paracrine effects and immunomodulative functions [19,60]. Hence, the increased migration of UCB-MSCs into a wound bed can enhance the factors involved in cutaneous wound-healing. Our results indicate that
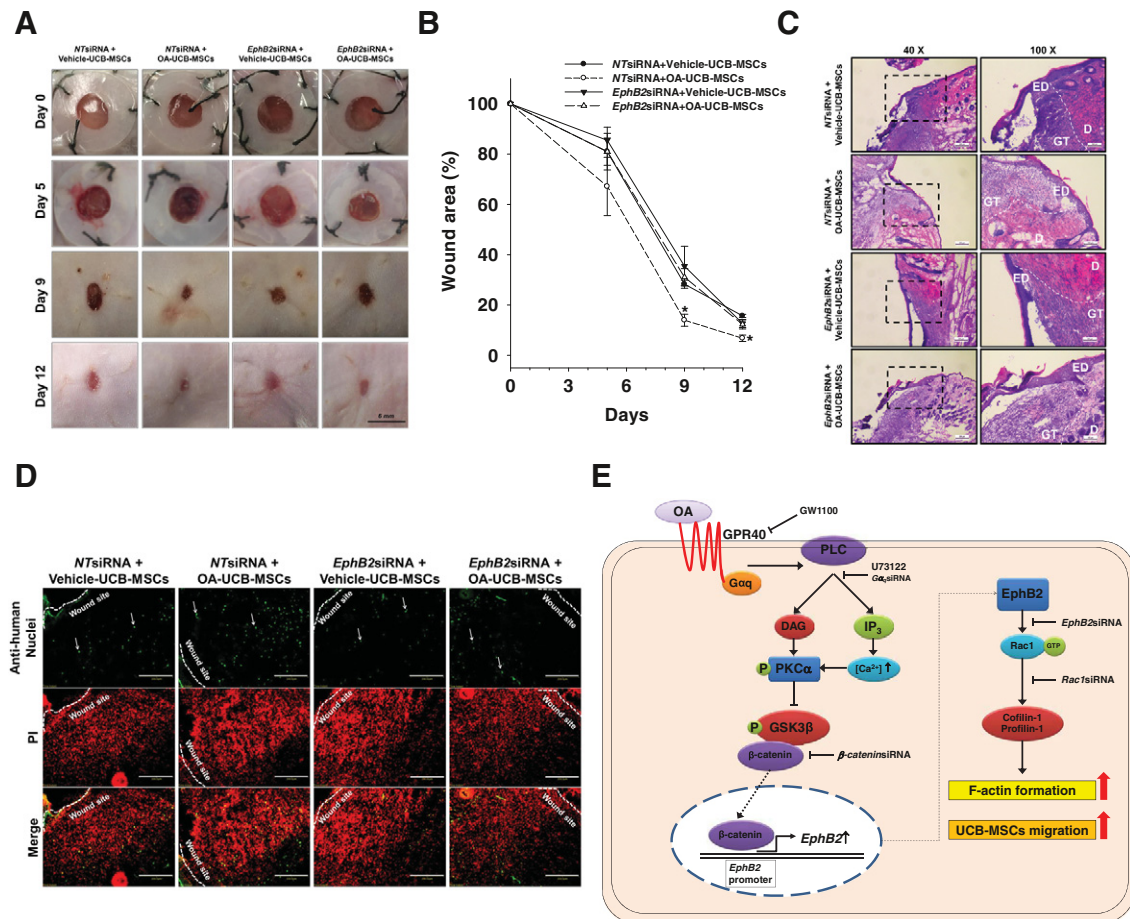

Fig. 6. OA-induced EphB2 expression enhances the skin wound-healing effect of UCB-MSCs. (A) Representative images of gross examination on skin wound-healing on days 0, 5, 9 and 12 are shown. n = 8. Scale bar, 6 mm. (B) Percentages of wound size relative to the initial wound size on days 0, 5, 9 and 12 are shown. n = 8. *$P < 0.05$ versus vehicle-treated NTsiRNA + UCB-MSCs. (C) On day 12, histological assessment was done by H&E staining. Representative images are shown. Scale bar, 200 μm (magnification, ×40) and 100 μm (magnification, ×100). ED, epidermis; D, dermis; GT, granulation tissue. (D) Detection of UCB-MSCs transplanted in the mouse skin wound was done by staining with anti-human nuclei antibody (MAB1281A4). Frozen sections were stained with Alexa Fluor® 488 conjugated anti-human nuclei antibody (Green) and PI (Red). The representative image of the human nuclei positive/PI positive is shown. Scale bar, 200 μm (magnification, ×200). (E) A proposed model for OA-induced signaling pathways in enhancing UCB-MSC motility.

the pre-activation of UCB-MSCs with an OA treatment can be useful in a wide range of stem cell therapies and can increase the rate of engraftment of UCB-MSCs.

4.1. Conclusion

Collectively, our results suggest that OA is a promising natural lipid metabolite, as it can promote the motility of UCB-MSCs, which results in the promotion of tissue regeneration. OA enhances UCB-MSC motility through EphB2-dependent F-actin formation involving the PKCα/GSK3β/β-catenin and Rac1 signaling pathway (Fig. 6E). Accordingly, an OA pretreatment can enhance the therapeutic potency of UCB-MSCs. In conclusion, we have identified EphB2 as a crucial factor in OA-mediated functions that improve UCB-MSC migration and therapeutic potency levels while also enhancing the skin wound-healing process.

Conflict of interest statement

The authors indicate no potential conflicts of interest

Transparency Document

The Transparency document associated with this article can be found, in the online version.

Acknowledgements

Appendix A. Supplementary data

Supplementary data to this article can be found online at http://dx.doi.org/10.1016/j.bbamcr.2015.05.006.

References

[1] H. Shapiro, S. Shachar, I. Sekler, M. Hershfinkel, M.D. Walker, Role of GPR40 in fatty acid action on the β cell line INS-1E, Biochem. Biophys. Res. Commun. 335 (2005) 97–104.

[2] J.X. Kang, J.B. Wan, C. He, Concise review: regulation of stem cell proliferation and differentiation by essential fatty acids and their metabolites, Stem Cells 32 (2014) 1092–1098.

[3] K. Ito, T. Suda, Metabolic requirements for the maintenance of self-renewing stem cells, Nat. Rev. Mol. Cell Biol. 15 (2014) 243–256.

[4] A.N. Smith, L.A. Muffley, A.N. Bell, S. Numhom, A.M. Hocking, Unsaturated fatty acids induce mesenchymal stem cells to increase secretion of angiogenic mediators, J. Cell. Physiol. 227 (2012) 3225–3233.

[5] J. Kinsella, Stearyl CoA as a precursor of oleic acid and glycerolipids in mammary microsomes from lactating bovine: possible regulatory step in milk triglyceride synthesis, Lipids 7 (1972) 349–355.

[6] C.R. Cardoso, S. Favoreto Jr., L.L. Oliveira, J.O. Vancim, G.B. Barban, D.B. Ferraz, J.S. Silva, Oleic acid modulation of the immune response in wound healing: A new approach for skin repair, Immunobiology 216 (2011) 409–415.

[7] F. Djelti, H. Merzouk, S.A. Merzouk, M. Narce, In vitro effects of oil's fatty acids on T cell function in gestational diabetic pregnant women and their newborns, J. Diabetes (2014)http://dx.doi.org/10.1111/1753-0407.12210 ([Epub ahead of print]).

[8] T. Nomura, C. Göritz, T. Catchpole, M. Henkemeyer, J. Frisén, EphB signaling controls lineage plasticity of adult neural stem cell niche cells, Cell Stem Cell 7 (2010) 730–743.

[9] M. Genander, J. Frisén, Ephrins and Eph receptors in stem cells and cancer, Curr. Opin. Cell Biol. 22 (2010) 611–616.

[10] M.G. Coulthard, M. Morgan, T.M. Woodruff, T.V. Arumugam, S.M. Taylor, T.C. Carpenter, M. Lackmann, A.W. Boyd, Eph/Ephrin signaling in injury and inflammation, Am. J. Pathol. 181 (2012) 1493–1503.

[11] A. Nakayama, M. Nakayama, C.J. Turner, S. Höing, J.J. Lepore, R.H. Adams, Ephrin-B2 controls PDGFRβ internalization and signaling, Genes Dev. 27 (2013) 2576–2589.

[12] U. Huynh-Do, C. Vindis, H. Liu, D.P. Cerretti, J.T. McGrew, M. Enriquez, J. Chen, T.O. Daniel, Ephrin-B1 transduces signals to activate integrin-mediated migration, attachment and angiogenesis, J. Cell Sci. 115 (2002) 3073–3081.

[13] H. Miao, D.-Q. Li, A. Mukherjee, H. Guo, A. Petty, J. Cutter, J.P. Basilion, J. Sedor, J. Wu, D. Danielpour, A.E. Sloan, M.L. Cohen, B. Wang, EphA2 mediates ligand-dependent inhibition and ligand-independent promotion of cell migration and invasion via a reciprocal regulatory loop with Akt, Cancer Cell 16 (2009) 9–20.

[14] A. Arthur, A. Zannettino, R. Panagopoulos, S.A. Koblar, N.A. Sims, C. Stylianou, K. Matsuo, S. Gronthos, EphB/ephrin-B interactions mediate human MSC attachment, migration and osteochondral differentiation, Bone 48 (2011) 533–542.

[15] E. Colletti, D. El Shabrawy, M. Soland, T. Yamagami, S. Mokhtari, C. Osborne, K. Schlauch, E.D. Zanjani, C.D. Porada, G. Almeida-Porada, EphB2 isolates a human marrow stromal cell subpopulation with enhanced ability to contribute to the resident intestinal cellular pool, FASEB J. 27 (2013) 2111–2121.

[16] J. Holmberg, M. Genander, M.M. Halford, C. Annerén, M. Sondell, M.J. Chumley, R.E. Silvany, M. Henkemeyer, J. Frisén, EphB receptors coordinate migration and proliferation in the intestinal stem cell niche, Cell 125 (2006) 1151–1163.

[17] J. Doleman, J. Eady, R. Elliott, R. Foxall, J. Seers, I. Johnson, E. Lund, Identification of the Eph receptor pathway as a novel target for eicosapentaenoic acid (EPA) modification of gene expression in human colon adenocarcinoma cells (HT-29), Nutr. Metab. 7 (2010) 56.

[18] M.A.J. Iafolla, J. Tay, D.S. Allan, Transplantation of umbilical cord blood–derived cells for novel indications in regenerative therapy or immune modulation: a scoping review of clinical studies, Biol. Blood Marrow Transplant. 20 (2014) 20–25.

[19] M. Wang, Y. Yang, D. Yang, F. Luo, W. Liang, S. Guo, J. Xu, The immunomodulatory activity of human umbilical cord blood-derived mesenchymal stem cells in vitro, Immunology 126 (2009) 220–232.

[20] S. Maxson, E.A. Lopez, D. Yoo, A. Danilkovitch-Miagkova, M.A. LeRoux, Concise review: role of mesenchymal stem cells in wound repair, Stem Cells Transl. Med. 1 (2012) 142–149.

[21] W.J. Ennis, A. Sui, A. Bartholomew, Stem cells and healing: impact on inflammation, Adv. Wound Care 2 (2013) 369–378.

[22] I. Rosova, M. Dao, B. Capoccia, D. Link, J.A. Nolta, Hypoxic preconditioning results in increased motility and improved therapeutic potential of human mesenchymal stem cells, Stem Cells 26 (2008) 2173–2182.

[23] S.-E. Yang, C.-W. Ha, M. Jung, H.-J. Jin, M. Lee, H. Song, S. Choi, W. Oh, Y.-S. Yang, Mesenchymal stem/progenitor cells developed in cultures from UC blood, Cytotherapy 6 (2004) 476–486.

[24] Y.S. Chang, S.J. Choi, S.Y. Ahn, D.K. Sung, S.I. Sung, H.S. Yoo, W.I. Oh, W.S. Park, Timing of umbilical cord blood derived mesenchymal stem cells transplantation determines therapeutic efficacy in the neonatal hyperoxic lung injury, PLoS One 8 (2013) e52419.

[25] L. Dunn, H.C. Prosser, J.T. Tan, L.Z. Vanags, M.K. Ng, C.A. Bursill, Murine model of wound healing, J. Vis. Exp. 75 (2013) e50265.

[26] B. Cox, A. Emili, Tissue subcellular fractionation and protein extraction for use in mass-spectrometry-based proteomics, Nat. Protoc. 1 (2006) 1872–1878.

[27] O. Salvucci, D. Maric, M. Economopoulou, S. Sakakibara, A. Follenzi, G. Tosato, EphrinB reverse signaling contributes to endothelial and mural cell assembly into vascular structures, Blood 114 (2009) 1707–1716.

[28] A. Stokowski, S. Shi, T. Sun, P.M. Bartold, S.A. Koblar, S. Gronthos, EphB/Ephrin-B interaction mediates adult stem cell attachment, spreading, and migration: implications for dental tissue repair, Stem Cells 25 (2007) 156–164.

[29] C.P. Briscoe, M. Tadayyon, J.L. Andrews, W.G. Benson, J.K. Chambers, M.M. Eilert, C. Ellis, N.A. Elshourbagy, A.S. Goetz, D.T. Minnick, P.R. Murdock, H.R. Sauls, U. Shabon, L.D. Spinage, J.C. Strum, P.G. Szekeres, K.B. Tan, J.M. Way, D.M. Ignar, S. Wilson, A.I. Muir, The orphan G protein-coupled receptor GPR40 is activated by medium and long chain fatty acids, J. Biol. Chem. 278 (2003) 11303–11311.

[30] B. Xue, M.L. Guo, D.Z. Jin, L.M. Mao, J.Q. Wang, Cocaine facilitates PKC maturation by upregulating its phosphorylation at the activation loop in rat striatal neurons in vivo, Brain Res. 1435 (2012) 146–153.

[31] J.L. Garrido, J.A. Godoy, A. Alvarez, M. Bronfman, N.C. Inestrosa, Protein kinase C inhibits amyloid β peptide neurotoxicity by acting on members of the Wnt pathway, FASEB J. 16 (2002) 1982–1984.

[32] S.L. Etheridge, G.J. Spencer, D.J. Heath, P.G. Genever, Expression profiling and functional analysis of Wnt signaling mechanisms in mesenchymal stem cells, Stem Cells 22 (2004) 849–860.

[33] E. Batlle, J.T. Henderson, H. Beghtel, M.M.W. van den Born, E. Sancho, G. Huls, J. Meeldijk, J. Robertson, M. van de Wetering, T. Pawson, H. Clevers, β-Catenin and TCF mediate cell positioning in the intestinal epithelium by controlling the expression of EphB/EphrinB, Cell 111 (2002) 251–263.

[34] S.D. Wang, P. Rath, B. Lal, J.-P. Richard, Y. Li, C.R. Goodwin, J. Laterra, S. Xia, EphB2 receptor controls proliferation/migration dichotomy of glioblastoma by interacting with focal adhesion kinase, Oncogene 31 (2012) 5132–5143.

[35] M. Sohl, F. Lanner, F. Farnebo, Sp1 mediate hypoxia induced ephrinB2 expression via a hypoxia-inducible factor independent mechanism, Biochem. Biophys. Res. Commun. 391 (2010) 24–27.

[36] S.S. Foo, C.J. Turner, S. Adams, A. Compagni, D. Aubyn, N. Kogata, P. Lindblom, M. Shani, D. Zicha, R.H. Adams, Ephrin-B2 controls cell motility and adhesion during blood–vessel–wall assembly, Cell 124 (2006) 161–173.

[37] Y. Wang, M. Nakayama, M.E. Pitulescu, T.S. Schmidt, M.L. Bochenek, A. Sakakibara, S. Adams, A. Davy, U. Deutsch, U. Luthi, A. Barberis, L.E. Benjamin, T. Makinen, C.D. Nobes, R.H. Adams, Ephrin-B2 controls VEGF-induced angiogenesis and lymphangiogenesis, Nature 465 (2010) 483–486.

[38] M.J. Chumley, T. Catchpole, R.E. Silvany, S.G. Kernie, M. Henkemeyer, EphB receptors regulate stem/progenitor cell proliferation, migration, and polarity during hippocampal neurogenesis, J. Neurosci. 27 (2007) 13481–13490.

[39] P. Jung, T. Sato, A. Merlos-Suarez, F.M. Barriga, M. Iglesias, D. Rossell, H. Auer, M. Gallardo, M.A. Blasco, E. Sancho, H. Clevers, E. Batlle, Isolation and in vitro expansion of human colonic stem cells, Nat. Med. 17 (2011) 1225–1227.

[40] C.P. Briscoe, M. Tadayyon, J.L. Andrews, W.G. Benson, J.K. Chambers, M.M. Eilert, C. Ellis, N.A. Elshourbagy, A.S. Goetz, D.T. Minnick, The orphan G protein-coupled receptor GPR40 is activated by medium and long chain fatty acids, J. Biol. Chem. 278 (2003) 11303–11311.

[41] J.-Y. Park, Y.M. Kim, H.S. Song, K.Y. Park, Y.M. Kim, M. Seon Kim, Y.K. Pak, I.K. Lee, J.D. Lee, S.-J. Park, Oleic acid induces endothelin-1 expression through activation of protein kinase C and NF-κB, Biochem. Biophys. Res. Commun. 303 (2003) 891–895.

[42] M. Shigeto, K. Kaku, Are both protein kinase A- and protein kinase C-dependent pathways involved in glucagon-like peptide-1 action on pancreatic insulin secretion? J. Diabetes Invest. 5 (2014) 347–348.

[43] A.D. Mancini, V. Poitout, The fatty acid receptor FFA1/GPR40 a decade later: how much do we know? Trends Endocrinol. Metab. 24 (2013) 398–407.

[44] Y. Shirai, N. Saito, Activation mechanisms of protein kinase C: maturation, catalytic activation, and targeting, J. Biochem. 132 (2002) 663–668.

[45] M. Ferdaoussi, V. Bergeron, B. Zarrouki, J. Kolic, J. Cantley, J. Fielitz, E.N. Olson, M. Prentki, T. Biden, P.E. MacDonald, V. Poitout, G protein-coupled receptor (GPR)40-dependent potentiation of insulin secretion in mouse islets is mediated by protein kinase D1, Diabetologia 55 (2012) 2682–2692.

[46] Y. Itoh, Y. Kawamata, M. Harada, M. Kobayashi, R. Fujii, S. Fukusumi, K. Ogi, M. Hosoya, Y. Tanaka, H. Uejima, H. Tanaka, M. Maruyama, R. Satoh, S. Okubo, H. Kizawa, H. Komatsu, F. Matsumura, Y. Noguchi, T. Shinohara, S. Hinuma, Y. Fujisawa, M. Fujino, Free fatty acids regulate insulin secretion from pancreatic β cells through GPR40, Nature 422 (2003) 173–176.

[47] S.-J. Lee, Y.H. Jung, S.Y. Oh, M.S. Yong, J.M. Ryu, H.J. Han, Netrin-1 induces MMP-12-dependent E-cadherin degradation via the distinct activation of PKCα and FAK/Fyn in promoting mesenchymal stem cells motility, Stem Cells Dev. 23 (2014) 1870–1882.

[48] B. Kasenda, S.H. Kassmer, B. Niggemann, S. Schiermeier, W. Hatzmann, K.S. Zänker, T. Dittmar, The stromal cell-derived factor-1α dependent migration of human cord blood CD34+ haematopoietic stem and progenitor cells switches from protein kinase C (PKC)-α dependence to PKC-α independence upon prolonged culture in the presence of Flt3-ligand and interleukin-6, Br. J. Haematol. 142 (2008) 831–835.

[49] S.F. Moore, M.T.J. van den Bosch, R.W. Hunter, K. Sakamoto, A.W. Poole, I. Hers, Dual regulation of glycogen synthase kinase 3 (GSK3)α/β by protein kinase C (PKC)α and Akt promotes thrombin-mediated integrin αIIbβ3 activation and granule secretion in platelets, J. Biol. Chem. 288 (2013) 3918–3928.

[50] S.J. Kühl, M. Kühl, On the role of Wnt/β-catenin signaling in stem cells, Biochim. Biophys. Acta Gen. Subj. 1830 (2013) 2297–2306.

[51] D. Mauvoisin, C. Charfi, A.M. Lounis, E. Rassart, C. Mounier, Decreasing stearoyl-CoA desaturase-1 expression inhibits β-catenin signaling in breast cancer cells, Cancer Sci. 104 (2013) 36–42.

[52] D.B. Nikolov, K. Xu, J.P. Himanen, Eph/ephrin recognition and the role of Eph/ephrin clusters in signaling initiation, Biochim. Biophys. Acta Protein Proteomics 1834 (2013) 2160–2165.

[53] A. Steffen, M. Ladwein, G.A. Dimchev, A. Hein, L. Schwenkmezger, S. Arens, K.I. Ladwein, J.M. Holleboom, F. Schur, J.V. Small, J. Schwarz, R. Gerhard, J. Faix, T.E.B. Stradal, C. Brakebusch, K. Rottner, Rac function is crucial for cell migration but is not required for spreading and focal adhesion formation, J. Cell Sci. 126 (2013) 4572–4588.

[54] C.H. Fernández-Espartero, D. Ramel, M. Farago, M. Malartre, C.M. Luque, S. Limanovich, S. Katzav, G. Emery, M.D. Martín-Bermudo, GTP exchange factor Vav regulates guided cell migration by coupling guidance receptor signalling to local Rac activation, J. Cell Sci. 126 (2013) 2285–2293.

[55] P. Penzes, A. Beeser, J. Chernoff, M.R. Schiller, B.A. Eipper, R.E. Mains, R.L. Huganir, Rapid induction of dendritic spine morphogenesis by trans-synaptic EphrinB–EphB receptor activation of the Rho-GEF kalirin, Neuron 37 (2003) 263–274.

[56] M. Abreu-Blanco, J. Watts, J. Verboon, S. Parkhurst, Cytoskeleton responses in wound repair, Cell. Mol. Life Sci. 69 (2012) 2469–2483.

[57] S.-W. Kim, H.-Z. Zhang, L. Guo, J.-M. Kim, M.H. Kim, Amniotic mesenchymal stem cells enhance wound healing in diabetic NOD/SCID mice through high angiogenic and engraftment capabilities, PLoS One 7 (2012) e41105.

[58] O. Salvucci, M.D.L.L. Sierra, J.A. Martina, P.J. McCormick, G. Tosato, EphB2 and EphB4 receptors forward signaling promotes SDF-1-induced endothelial cell chemotaxis and branching remodeling, Blood 108 (2006) 2914–2922.

[59] E.B. Pasquale, Eph receptors and ephrins in cancer: bidirectional signalling and beyond, Nat. Rev. Cancer 10 (2010) 165–180.

[60] J.A. Ankrum, J.F. Ong, J.M. Karp, Mesenchymal stem cells: immune evasive, not immune privileged, Nat. Biotechnol. 32 (2014) 252–260.